Flight Electronics of GC-Mass Spectrometer for Investigation of Volatiles in the Lunar Regolith

Rico G. Fausch
University of Bern, Physics Institute
Sidlerstrasse 5
3012 Bern
+41 31 631 44 16
rico.fausch@space.unibe.ch

Peter Wurz
University of Bern, Physics Institute
Sidlerstrasse 5
3012 Bern
+41 31 631 44 26
peter.wurz@space.unibe.ch

Marek Tulej
University of Bern, Physics Institute
Sidlerstrasse 5
3012 Bern
+41 31 631 55 46
marek.tulej@space.unibe.ch

Jürg Jost
University of Bern, Physics Institute
Sidlerstrasse 5
3012 Bern
+41 31 631 44 55
juerg.jost@space.unibe.ch

Pascal Gubler
University of Bern, Physics Institute
Sidlerstrasse 5
3012 Bern
+41 31 631 41 07
pascal.gubler@space.unibe.ch

Mario Gruber
University of Bern, Physics Institute
Sidlerstrasse 5
3012 Bern
+41 31 631 44 49
mario.gruber@space.unibe.ch

Davide Lasi
University of Bern, Physics Institute
Sidlerstrasse 5
3012 Bern
+41 31 631 44 29
davide.lasi@space.unibe.ch

Claudio Zimmermann
University of Bern, Physics Institute
Sidlerstrasse 5
3012 Bern
+41 31 631 34 21
claudio.zimmermann@space.unibe.ch

Thomas Gerber
University of Bern, Physics Institute
Sidlerstrasse 5
3012 Bern
+41 31 631 44 54
thomas.gerber@space.unibe.ch

Abstract—**We introduce electronics designed to control measurement cycles performed with the compact neutral gas mass spectrometer (NGMS), which is a time-of-flight (TOF) system. NGMS is combined with a gas chromatograph (GC) and a pyrolysis oven to form a gas analytic complex on board the Russian Luna-Resurs spacecraft to land on the Moon. The instrument will investigate chemical composition of the soils at lunar polar regions and the tenuous lunar exosphere. NGMS measures the elemental, isotopic and molecular composition of gaseous samples including CHON compounds, water and noble gases, by recording TOF spectra that are converted to mass spectra during data analysis. Our miniature mass spectrometer has a robust and modular design. It combines an ion storage source with redundant thermionic electron emitters, a pulsed ion extraction for ion acceleration, ion drift path, ion mirror, a second ion drift path, and a high-speed microchannel plate detector. Starting from the ion source where species are ionized and the consecutive mass separation in the field free regions of a TOF section, ion packages arrive some micro-seconds later at the multichannel ion detector. The detector produces current pulses with peak widths of nanoseconds allowing for measurements with a high mass resolution in spite of a short drift tube length. During test measurements, we achieved mass resolution > 1000 together with a dynamic range of up to 10^6 within 1 second integration time. Hence, the instrument depends on high electric field strengths in the ion-optical system and a high-speed and low-noise data acquisition system resulting in highly customized control electronics. We developed the complete electronic system complying with the mission requirements (power consumption of 25 watt maximum, size, mass and radiation tolerance) for controlling the instrument operation and acquiring data from this complex analytical package. Given the heritage from LASMA/Phobos-Grunt, CaSSIS/Exo-Mars, RTOF/Rosetta and P-BACE/MEAP missions, the presented design demonstrates that NGMS is capable to investigate chemical composition with allocated resources of power and size. Our flight-proven control unit operating NGMS represents a reliable system for further similar applications as the Neutral Gas and Ion Mass spectrometer NIM/PEP on board ESA's JUICE mission.**

TABLE OF CONTENTS

1. INTRODUCTION

The neutral gas mass spectrometer (NGMS) is a scientific instrument selected for the Russian Luna-Resurs mission to measure chemical composition of the regolith at the lunar surface and tenuous exosphere in situ. The NGMS instrument is part of the Gas Analytic Package (GAP), which further includes a pyrolysis oven and a gas chromatograph (GC).

GAP will perform chemical composition measurements including molecular composition of volatiles (CHON compounds, water), as well as the isotope composition of noble gases in the lunar regolith to help in our understanding of the origin and evolution of the Moon and of the solar system within a larger context.

Presently available lunar samples originate from a restricted region near the lunar equator of the lunar near side, with

exception of lunar meteorites, whose origin on the lunar surface is likely more widespread but unknown [1]. Therefore, the Luna-Resurs mission targets a landing site near a crater with permanent shadow near the southern pole. The overall science requirements of the Luna-Resurs mission [2] are designed to enhance our understanding of the origin and evolution of solar system bodies.

As solar input for the lander is limited on the poles, energy efficiency is crucial for the lander. Even more important, the lander mass has to be considered carefully to perform landing on the Moon. Consequently, mass, size and power allocated to all parts of the lander system are challenging and design driving factors regarding mechanics and electronics. Small mechanics result in large efforts to design the electronic control and acquisition system. Saving power and reducing size of electronics compared to previous missions [3] at once demand new concepts for the instrument. Detailed specifications of NGMS instrument and scientific background are discussed in [4, 5] and references therein.

The NGMS instrument is a compact Time-Of-Flight (TOF [6]) mass spectrometer designed to analyze gaseous samples in situ. It has two major scientific operation modes. In exosphere mode, the NGMS instrument measures directly gases of the lunar exosphere from the location of the lander, while inserted into artificial Moon satellite orbit and on the lunar surface. In gas chromatograph mode, the pyrolysis oven releases volatiles from collected soil samples with temperatures of up to 1000°C, which are either separated by the GC and further analyzed by the NGMS, or directly analyzed by the NGMS. A drill unit on the lander provides soil samples of the upper lunar soil down to 1 meter depth to the pyrolysis oven, where they are heated. The released volatiles are transported from the pyrolysis oven to the GC unit by means of He carrier gas. In the GC instrument, the compounds are chemically separated with respect to time depending on their retention in the GC columns. The output of the GC is a continuous gas flow of the carrier gas with a sequence of molecules and elements of the introduced sample. Different species arrive at the output of the GC at different times depending on their retention times. Peak widths in GC time space are of the order of seconds. This leads to a desired sampling frequency of the GC output in the range of 0.1–1 seconds for the integration time of mass spectra.

Mass spectrometers based on the TOF principle allow for acquiring a complete mass spectrum at once without scanning over the mass range. Neutral gas from GC or exosphere is ionized in the ionization chamber of the ion source by electron ionization (EI). TOF instruments are pulsed instruments. To overcome the duty cycle from the pulsing and therefore increase the sensitivity of NGMS, the instrument features an ion storage source (IOS), where the continuously produced ions are stored until ion extraction into the TOF system [7]. Pulsed ion extraction by the primary pulser (PP) and further acceleration to the drift energy pulls the ion cloud into the first drift path, where it separates along a TOF trajectory into ion packages according to their mass-to-charge ratio. Pulsed ion extraction is performed with 10 kilohertz repetition rate during nominal operations. At the end of the drift tube, there is a grid-less ion mirror and a second pulsed electrode. In GC-mode, the secondary pulser (PS) removes the ions from the GC carrier gas to prevent the detector from saturation. Flight trajectories of other ions are not influenced as they pass the ion reflection zone before or after PS is operating. Electric interference (EMC) introduced by the PS needs to be minimized, as the mass range of influence of the PS needs to be restricted. Ions outside the PS operating time continue their trajectories and further separate in time during their passage of the second drift tube before reaching the detector. The detector is a high-speed microchannel plate (MCP) detector system with impedance matched anode [8]. Spectra are received in the time domain and easily converted into mass-to-charge spectra during data analysis. The data acquisition system (DAQ) digitizes the output of the MCP detector and converts the current pulses into voltage peaks. All signals generated from one ion extraction represent a single-shot spectrum, a waveform. Waveform summation over a given period of time, the integration time, results in a histogram (time spectrum), which is then stored. All the spectra of a measurement cycle need to be stored locally in the instrument until transmission to Earth is possible by the spacecraft. A typical mission scenario foresees ground communication with the spacecraft once an Earth day to fetch accumulated scientific and housekeeping (HK) data. Mission duration on the lunar surface is at least one lunar day, ideally up to five lunar days. Acquiring measurements on the surface is foreseen during lunar day while the spacecraft is likely to provide a temperature range from –40°C to +35°C.

Mass of the NGMS instrument is < 3.5 kg and maximum size is 26 x 15 x 18 cm^3. The compact length of the NGMS instrument influences the requirements on electronics, e.g. sampling rate of the digitizer. Because all ions are accelerated to the same energy in the ion source, the mass resolution of the TOF mass spectrometer $R = m/\Delta m$ is given by $R = t_{TOF}/2\Delta t$, where t_{TOF} is the mean TOF of an ion package of mass m/z and Δt is the peak width of the corresponding ion package recorded by the detector. The longer the drift path is the larger t_{TOF} becomes, and the more the ion packages separate. Given the limited size allocated for space-born instruments, t_{TOF} is short and therefore the ion package length in time, Δt, has to be rather small to achieve the necessary mass resolution. For a mass resolution of up to $m/\Delta m = 1100$, which results from the requirement to quantitatively analyze isotopic compositions and identify hydrocarbons [5], digitization of the detector signal at 2 Gs/s results, for which the electronics is optimized. Narrow ion package peak widths result in better separation of masses. In addition, a fast high-voltage pulser is necessary to achieve the resolution of the mass spectrum with an otherwise optimized ion-optical system. A consequence of the narrow peaks is the need for a fast data acquisition.

Solar power input for the lander is limited on the poles and therefore available electric power needs to be used efficiently. For the NGMS instrument, the allocated maximum power is 25 watt for nominal operations, while during standby mode it is < 6.8 watt. Among other things, the power consumption of the fast high-voltage pulsers and the high-speed DAQ system were highly optimized, and care was taken for a highly energy efficient power system. These were some of the main achievements of the design of the instrument's electronics.

2. Design and Methods

The NGMS instrument is divided into two major functional parts: The sensor that is the ion-optical system, which includes the ion source, ion optics and detector (Figure 1). Electronics (Figure 1, 2) control the sensor, provide electric power and perform communication between the NGMS instrument and the data-handling unit of the spacecraft (BUNI). Both parts benefit from earlier developments: RTOF/Rosina/Rosetta [3], P-BACE/MEAP [9], LASMA/Phobos-Grunt [10] and CaSSIS/ExoMars [11]. Figure 3 presents an overview of the functional elements of the electronics design. Electronic hardware consists of three PCB boards. Power electronics is located on the power board and the high voltage pulser board. The mainboard hosts the digital and data acquisition units of electronics. Power and main board are located in the main electronic box. To reduce the EMC disturbance created of the high voltage pulsers, the pulser board is located in an external housing in proximity to the pulsed electrode.

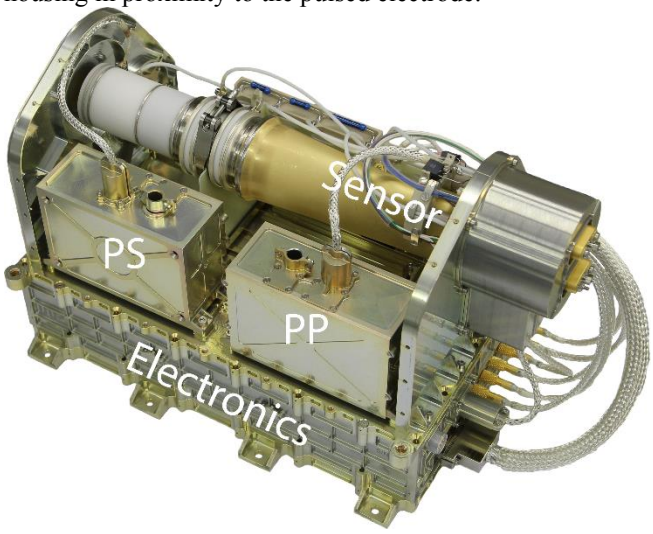

Figure 1. The flight model of the NGMS instrument. Pulser boxes (primary and secondary) are at prototype level, and therefore two boxes are visible. They are combined into a single print for the flight model. The lower part houses the rest of the electronics.

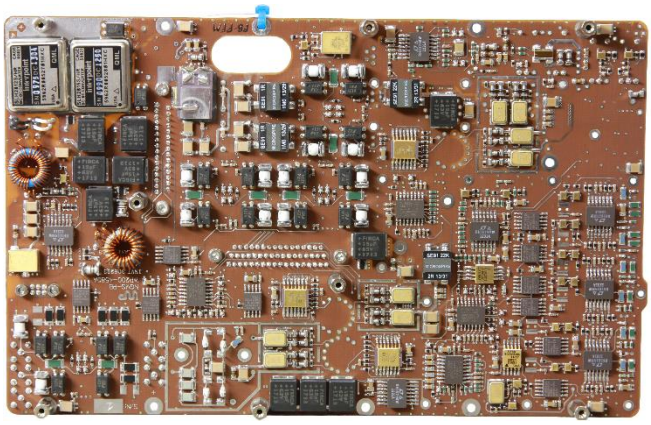

Figure 2. Sample electronic board of flight electronics during assembly phase. Main and power board are stacked to fit in the main electronic box.

Main Controller and Digital Design

Digital electronics is based on fault-tolerant Gaisler LEON3FT soft core processor embedded in a XILINX Virtex-4 FPGA. The space-qualified Virtex-4 is operated at 125 megahertz, and the soft core runs at 25 megahertz clock speed. The FPGA is controlling the peripheral drivers via Serial Peripheral Interface (SPI) busses (see Figure 3). A high-speed 10-bit ADC clocked at 2 gigahertz acquires TOF spectra continuously based on the trigger by the extraction pulser. It receives the detector signal via an impedance matched pre-amplifier stage and a low pass filter. Upon trigger, the ADC digitizes the signal for the duration of a TOF spectrum length. The data are passed to the FPGA for histograming TOF spectra over the integration time via a fast BRAM buffer system of the Virtex-4. Histogrammed spectra are then stored into flash memory for later download to ground.

An Advanced Microcontroller Bus Architecture (AMBA) consisting of an advanced peripheral bus (APB) and an advanced high-speed bus (AHB) interconnects peripheral modules to the LEON3FT CPU. The fault-tolerant memory controller interfaces to external 8 mebibytes (MiB) MRAM and to external SRAM via a 32+8 bit data-bus. The flash memory controller connects to an external flash device via an isolated 8-bit data-bus. Multiple SPI busses running with different speeds control external DAC and ADC devices for housekeeping collection and voltage control. The FPGA design is organized into modules, each dedicated to operate a certain part of the hardware like high voltage pulser, filament, sensor heating, sensor low and high voltages, high-speed ADC to sample the detector signal, and the spacecraft interface.

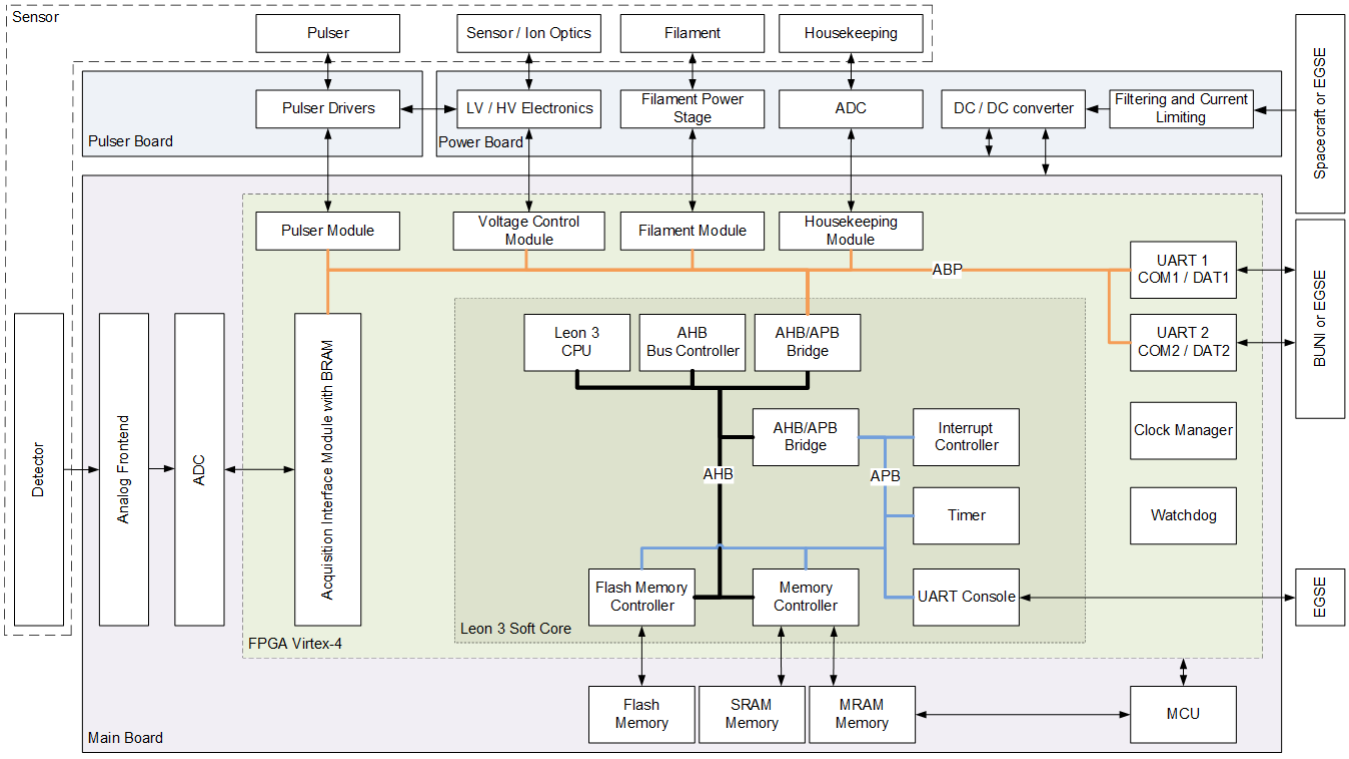

Figure 3. Block diagram of neutral gas mass spectrometer electronics. The system contains three boards on which units for signal processing and sensor controlling are integrated. An FPGA with an implemented microcontroller system controls the periphery integrated on the power and pulser board. Different FPGA units are connected with AHB and APB bus. The power board provides power to different boards where needed. Connections from low and high voltage electronics to the different boards are omitted for simplicity.

The configuration of the FPGA, its monitoring and the boot sequence requires a separate controller and external memory. As the Virtex-4 device only supports legacy one-time programmable memory devices (PROMs) to configure itself after power on reset (POR), an external radiation tolerant Atmel ATmegaS128 micro computing unit (MCU) is used to stream the configuration from the reprogrammable MRAM. Besides the configuration bit-stream for the FPGA, the MRAM holds the application firmware of the LEON3 CPU. Having a reprogrammable code source for the FPGA allows for much more flexibility in the software development at lower cost than the boot PROM solution.

The MCU boots from internal flash memory. Once the MCU runs, it loads the FPGA configuration image into the FPGA and releases the FPGA from its reset state. Upon reset, the LEON3 runs a bootloader from MRAM to copy its application firmware from MRAM to SRAM and transfers execution to SRAM. The FPGA requires no further access to MRAM afterwards.

Housekeeping data of all relevant peripheral modules inform about the present state of the instrument. The HK ADCs are located on the electronic boards (mainboard and power board), and connected to the FPGA via several SPI busses. FPGA is capable to check a maximum of 56 crucial system parameters like voltage, currents and temperatures at 1 kilohertz, which are digitally low-pass filtered. The main controller sets the system into a protective state in case of HK limit violations. Overvoltage and overcurrent protection catch an event within < 10 milliseconds. In case of an event, voltages for consumer modules are switched off, latest HK data are collected and transferred to BUNI.

NGMS receives tele-commands and timecodes from BUNI over one line of the redundant command RS485 link (125 Kbit/s), and transfers HK and science data products to BUNI on both lines of the redundant data RS485 link (1 Mbit/s).

Power Control Design

The NGMS electronic system creates its own DC voltages needed for operation on secondary side, as spacecraft provides +27 volt with a maximum of 25.0 watt on the primary side. On the primary side, common-mode chokes prevent from radio frequency and electromagnetic interference followed by a Latch Up Current Limiter (LCL) protecting instrument electronics and spacecraft form over current. Filters damp noise and distortions. Input voltages and currents are filtered as well.

DC/DC converters provide voltages for analogue and digital instrument electronics on the secondary side. Opto-couplers and transformers serve as galvanic separation between the primary spacecraft and the secondary side.

Sixteen independent voltages allow for an operation of the instrument according to the current environment. Temperature compensated Low Voltage (LVPS) and High Voltage Power Supplies (HVPS) both use two-stage DC/DC converters. Nine LVPS allow IOS and ion mirror voltage configuration between ±100 volt. However, rails of voltages are restricted according to the needs in the IOS to save power (see Table 1). Ion optics, high voltage pulsers and the detector require nine high voltages up to –5 kV. To safe further power, only seven HVPS with following voltage divider provide the voltages. The 12-bit resolution ensures a step size small enough to tweeze the instrument. All power supplies are designed to operate with low load and may operate as source or sink.

Table 1. Rails of the low and high voltage power supplies with its step size derived from their DAC.

Power Supply	Lower Rail / V	Upper Rail / V	Step Size / V
LVPS1	–100	100	0.049
LVPS2,4,5,7,9	–100	0	0.024
LVPS3,8	0	100	0.024
LVPS6	0	5	fixed
HVPS1,7	–5000	0	1.221
HVPS2,3	–2700	0	0.659
HVPS4	–600	0	1.000
HVPS5,6	–3200	0	0.781

High-Voltage Pulser Control Unit

A high-voltage pulser switches the voltage applied to an electrode of the ion-optical system between LVPS and HVPS (–600 volt) within nanoseconds rise time to the needed HV potential. Two pulsers are available and each one has its own LVPS but the same HVPS voltage. The clock of the primary pulser (defining the repetition rate) triggers the secondary pulser, when used, and the data acquisition. Rise time of the primary pulser is 3.3 nanoseconds. The rise time of secondary pulser pulses is slightly slower to reduce EMC induced into the drift tube. Repetition rate, both pulse widths, the delay between the pulses and the delay between primary pulse and data acquisition are adjustable.

Filament Control Unit

Ionization of molecules in the ion source is realized by electron ionization. Thermionic electron emission is a well-established technology to create an electron beam and consist mainly of a thin metallic wire, which is heated until electron emission occurs. Given the highly non-linear relation between electron emission and heating current of the filament [12], a fast and stable control loop is needed to maintain constant electron emission.

Therefore, this control loop consists of control circuitry in the FPGA and the filament power stage including a two-stage proportional-integral (PI) controller operating at 30 kilohertz. At this frequency neither the ion storage source nor the data acquisition are influenced. The filament controller operates with two control loops, with the inner loop controlling the heating current and the outer loop controlling emission current. As electron emission is essential for functionality of the instrument, NGMS implements two redundant filaments with its drivers.

Heating of the capillary bringing the sample gas from the GC system and the gas inlet itself is crucial to avoid condensation of gas inside the capillary and the ion source. A dedicated heating resistor is included in the instrument. To maintain a commanded temperature, the heater driver heats the ionization region of the ion source with up to 3.0 watt with a PWM signal applied to the heating resistor.

High-Speed Data Acquisition

An incoming ion package creates charge pulses on the detector leading to voltage peaks of nanoseconds length. Therefore, the system has to be capable to acquire data at 2 gigahertz sampling frequency. The detector signal line is terminated into 50 ohm to prevent signal reflection. The front-end signal input line is split up into two acquisition paths with different gain. High gain and low gain mode. This allows to adapt dynamic range and sensitivity of the acquisition system according to the measurement situation.

After low pass filtering of the input signal (to assure Nyquist frequency limit), the 10-bit TI ADC10D1000 continuously samples the signal in double edge sampling (DES) mode. Digitised data are sent via low voltage differential signaling (LVDS) to the FPGA, where it is temporarily stored into the 552 kibibyte of fast BRAM. To reach higher signal-to-noise ratios and reduce total data volume, the acquired waveforms are histogrammed during a programmable integration time. Once a histogrammed spectrum is completed, it is stored into 2 gibibyte NAND flash memory.

Flash access time limit the repetition rate of the histogram acquisition. Accounting transfer of page data from the FPGA to the flash device, the limitation is defined by the time needed by the flash to program ~4 kibibyte page data to memory cells. Thanks to the flash controller in the FPGA, we optimized time consumption, using two-plane page programming. The transfer takes only about 50 milliseconds, which provides enough margin to handle interfaces of higher priority in parallel. The implemented double buffer system ensures continuous data acquisition. Downloading spectra of a measurement campaign is possible either uncompressed or compressed with SPIHT

algorithm [13], that has been customized to optimize the compression for the histogrammed TOF spectra.

Debugging

Electrical Ground Support Equipment (EGSE) completely simulates BUNI and implements debugging access to the internal bus architecture of the FPGA. EGSE software allows for sending all commands, monitoring housekeeping data and acquired spectra, which are logged and displayed.

Radiation Mitigation

Local shielding of radiation sensitive parts assists software radiation mitigation where necessary. Based on the forecasted radiation environment on the Moon, the short mission duration of at most five lunations, and the implemented shielding the radiation hardness of the used electronic components has been outlined to be at least 30 kRad of total ionized dose (TID). Calculation of the probability of single event effects (SEU) in the microcontroller and the FPGA yields one event every 10 days. To mitigate impact and risk of single event upsets the FPGA registers are implemented with triple mode redundancy (TMR) and scrubbing of the FPGA configuration frames is performed continuously. Error detection and correction codes (EDAC) on the SRAM memory, block memory (BRAM) and CPU cache are implemented to further improve reliability of the digital electronics.

Measurements

We acquired mass spectra of residual gas during the first instrument commission session with different waveform accumulation numbers at two temperature levels to characterize the behavior of noise in spectra. For the cold case the temperature of the base plate, where the instrument is mounted on, and which simulates the boundary to the spacecraft, is –40°C and for the hot case it is +40°C. The vacuum chamber showed a pressure of $2.71 \cdot 10^{-8}$ millibar for the cold case and $5.06 \cdot 10^{-7}$ millibar for the hot case. Additional atmospheric gas is added to the vacuum chamber to achieve higher pressure in the hot case. We optimized the voltage set of the ion-optical system manually for the cold case and adapted only the MCP voltage and drift tube voltage for the hot case. Filament emission current was set to 200 microampere.

The numbers of accumulated waveforms commanded to the instrument represent typical operation cases. Ten spectra were acquired for each temperature case and waveform accumulation number. Corrupt spectra were excluded from data analysis when necessary. A custom made data analysis software converts time-of-flight spectra into mass spectra and calculates the window positions to extract the signals of the mass peaks. For our studies, we decided to analyze m/z 44 where the CO_2 molecule appears. After offset correction, the root mean square (RMS) of the voltage signal is divided by the RMS of the noise signal, which is measured at the end of the spectrum where currently no mass peaks appear. Because we are interested in the voltage peaks in the recorded waveforms, we define this amplitude ratio as SNRv, which equals the square root of the commonly used power signal to noise ratio (SNR).

3. Results and Discussion

Measurement Duration and Accumulation Time

The waveform integration time directly influences the maximum measurement durations. In exosphere-mode, a waveform accumulation time of 100 to 300 seconds is foreseen for integration, i.e., the summation of 1 million TOF spectra. The integration time, or rather the number of accumulations, is limited by the memory size of the buffer system in the FPGA (BRAM). In GC-mode, however, the integration time is given by the needed GC peak resolution that results in integration times of 0.1–1 seconds for NGMS, which are needed to optimally reconstruct GC peaks [14]. Integration time and pulser frequency are both variable. The primary pulser extracts ions nominally with 10 kilohertz and 10000 waveforms are integrated leading to 1-second waveform accumulation time in the buffer system.

Considering the horizontal resolution of 16-bit and the ADC sampling frequency, an upper boundary of recordable waveform length of 32.768 µs is given. This corresponds to an upper mass range of about $m/z \approx 1200$, which could be extended by adding more memory. However, the useful mass range is often considered to be given by the mass resolution, thus $m/z \lesssim 1000$, thus compatible with the allocated memory.

As the ADC has a vertical resolution of 10-bit, a spectrum in GC-mode with 1-second integration time contains 192 kibibyte of scientific data. This corresponds to more than 2 hours of measurements until the allocated flash memory is filled with uncompressed data. Thus, a GC-NGMS measurement cycle needs to be completed within this time. Therefore, heating profiles in the GC instrument need to be adapted to avoid extended retention time ranges. GC-NGMS measurements performed with the prototype GC-NGMS system [14] showed that accumulation time for the GC-mode can be reduced due to the GC peaks appearing at the gas chromatograph at much shorter times.

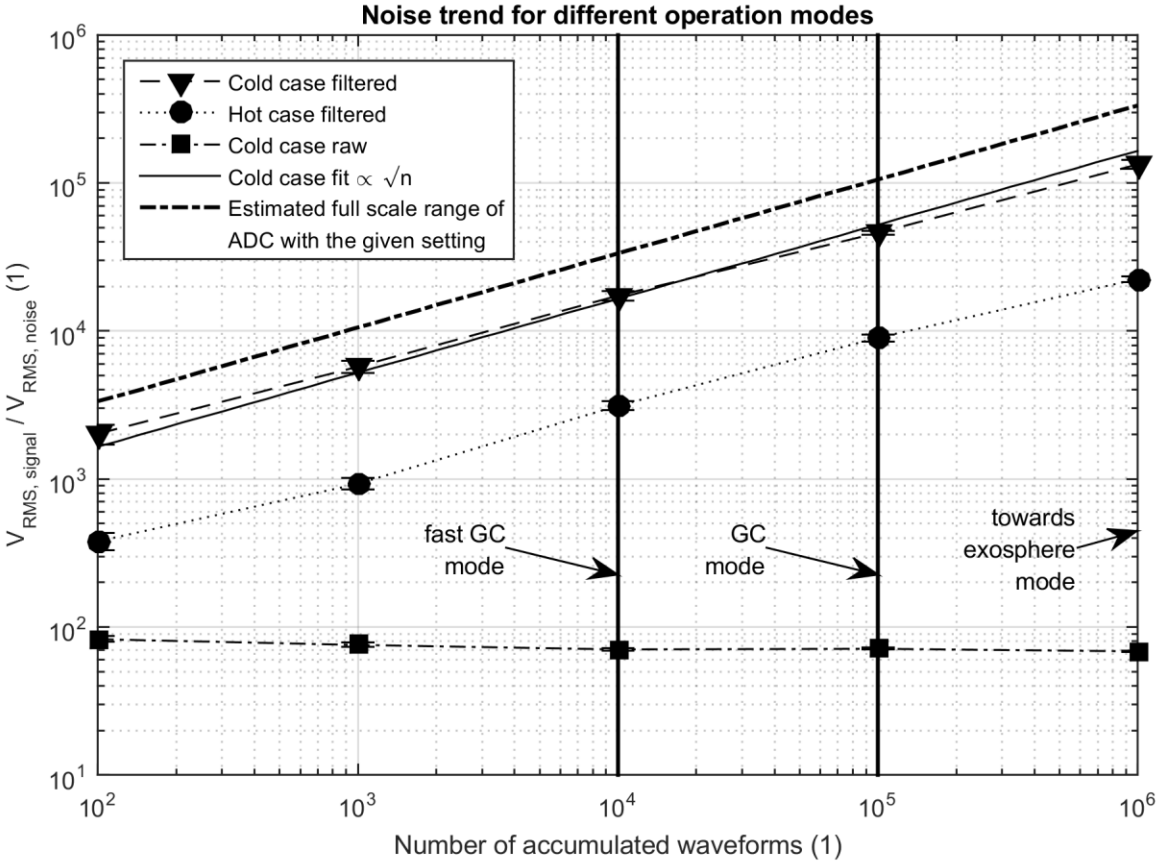

Figure 4. Amplitude ratio SNRv follows random noise after filtering. Harmonics limit SNRv in the spectra.

At the same time, the integration time has to be reduced at the beginning of the GC sequence to resolve the shortest GC peaks well. An increase of the sampling frequency of the GC output (decrease of the NGMS integration time) causes a reduction of the maximum duration of the measurement campaign given the allocated memory size (see Table 2). Electronics is, however, easily capable to adapt to the requirements inferred by the GC.

Noise Due to Mixed Board Design

In our measurements we can distinguish two major sources of noise in the waveform acquisition system, random noise and harmonic noise. Harmonic noise arises from cross talk from oscillators of the electronics to the front-end electronics and limit SNR of raw spectra to 37.6 decibel on average (Figure 4, cold case raw), independent of the number of accumulations. The random noise is assumed to be a Gaussian distribution, thus the SNRv should scale with the square root of the number of independent measurements. However, SNRv values stay constant at 74±6 for raw spectra over the measurement range of 10^2 to 10^6 accumulated waveforms, meaning that the noise adds itself in the same way to a spectrum as a signal does. This is true when harmonic noise dominates the noise because of mixed board design.

Incoming ions on the detector are amplified by a gain of about 10^6 in the detector resulting in millivolt pulses for a recorded ion, and being proportional to the number of ions registered on the detector in a time sampling bin. Thus, the waveform signal from the detector can be considered perfectly repetitive, while the ion signal is stable, and the SNRv should increase proportionally to the square root of the number of accumulated waveforms if the noise would be perfectly random.

Table 2. Buffer system leads to maximum measurement durations. Accumulation time can be chosen by software. Different configurations are indicated.

Proposed Mode	TOF Max.	Typical Accumulation Time	Max. Measurement Time
GC-Mode fast	32.7 µs	0.1 s	13 min
GC-Mode regular	32.7 µs	1 s	2 h 16 min
Exosphere-Mode	32.7 µs	100 s	11 h 33 min

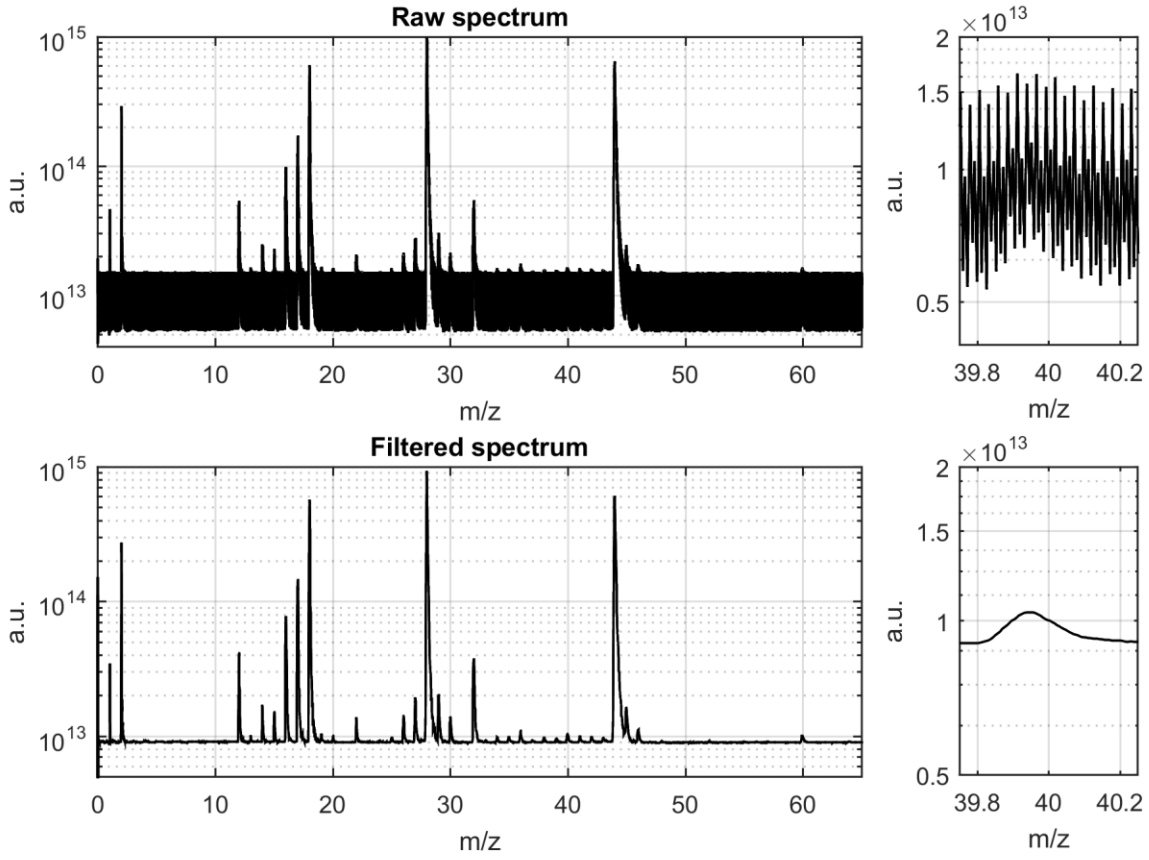

Figure 5. Mass spectra of raw and filtered data of residual gas (cold case) with 10^5 integrated waveforms (GC-mode) indicate the increased SNR after filtering. Harmonics are clearly visible in the upper right panel.

The limited volume and weight available for the electronics of the NGMS instrument leads to a non-optimal placement of electronic functional units with respect to noise minimization. They are only partially separated on different boards containing essential shielding only. Proximity of low- and high-speed circuits as well as mixing of analog and digital electronics lead to parasitic coupling effects. As the clocks on the boards are synchronized with the acquisition and sampling clock, fundamental and higher harmonic frequencies appear almost perfectly correlated to the measurement sampling times and will not average out with increasing number of accumulations, which explains the constant SNRv values for the range of accumulated waveforms.

Harmonic Noise Reduction

However, by post-acquisition filtering we can reduce the noise content in the waveforms already reasonably. To increase SNRv three types of filters were applied to the raw spectrum. Filtering in the frequency domain where clock signals are visible as distinct peaks reduce most of the noise present. Single frequencies are scaled and normal infinite impulse response (IIR) filter notch filters are placed around clock frequencies and multiples of them. Low pass filtering with a cut-off frequency near the bandwidth of the ADC around 500 megahertz (depending on the operation mode) and a weak moving average filter decrease noise additionally. Filtered spectra show significantly increased SNRv, as shown Figure 4, (hot case filtered and cold case filtered). The SNRv of the filtered waveforms follows the expected random Gaussian noise curve (Figure 4, cold case fit). In the cold case for 10^5 accumulated waveforms (1-second accumulations for the GC-Mode) the SNRv has increased to $(4.61\pm0.13)\cdot10^4$ or a SNR of 93.3 decibel. Other dominant mass peaks in the same spectra achieve similar SNR. The maximum limit of the SNR considering the full usable ADC range of 9 bits is 101 decibel.

Adapting to the Environment

Hot case measurements demonstrate the importance of optimizing the voltage set applied to the ion optical system. Mechanical elements expand slightly with increasing temperature leading to a slight distortion of the ion optics. A reduction in the signal could be compensated partially with a higher MCP voltage but this also yields more noise in the detector, and thus in data acquisition chain. These effects dominate over the increase of random noise arising in electronics and in the detector system. As hot case

measurements show in Figure 4, the uncorrected thermal influence reduces the SNRv about a decade but the instrument performs constant over time. This indicates the potential of the instrument with dedicated fully autonomous voltage set optimizer.

Optimization mainly includes finding an optimal voltage set for the ion optical system. This optimization is necessary to reach best performance because the data processing unit only knows the voltages as digital values, and the conversion to physical voltage changes with temperature. Changing voltages on electrodes influences the quality of the acquired spectrum. The optimizer analyses the TOF spectra, rates them based on a merit function, and defines a new voltage set according to an adaptive particle swarm algorithm [15, 16]. After optimization, the system is ready to perform stand-alone or together with the GC in measurement campaigns. As measurements were performed during early commissioning phase, an optimizer of this type was not ready then.

Scientific Context of Measurements

The NGMS instrument provides a suitable dynamic range to measure even trace quantities of species in the lunar environment. Figure 5 shows a typical mass spectrum of the measurement series with 1-second waveform accumulation time representative for the GC-Mode. The filtered spectrum features Gibbs overshoots to illustrate the consequences slight over filtering on mass resolution. It has to be noticed that the applied definitions of the SNR are not suitable to determine exact instrument detection limits rather than an estimation of the order of magnitude [20]. In a previous study reporting on the prototype of the NGMS instrument with more dedicated measurements and different SNR definitions, a lower limit of the dynamic range was demonstrated to be 10^6 for 1-second of integration time [14]. Results of the present study are comparable to [14], taking the different definitions of the SNR into account. We conclude that the dynamic range is in a comparable range. Therefore, in exosphere-mode, where low ambient gas pressure of the lunar atmosphere of the order of 10^{-10} millibar [6] a dynamic range of $> 10^6$, which seems to be possible with this instrument, leads to detection limits for partial pressures down to around 10^{-16} millibar.

Resource Compliance

The energy efficient design owes mainly to the development of the power control design. A significant reduction of the power consumption was achieved by building customized low-voltage and high-voltage power supplies. Additional power-saving measures, like the power consumption of the fast high-voltage pulsers, the high-speed DAQ system, and the filament controller were highly optimized. The system described allows operation of the instrument at < 25 watt. Nominal power consumption depends on the operation mode (see Table 3). These values are, however, upper limits, depending, e.g. on the required heating power in GC-mode. Exosphere-mode operation consumes less power as heater and secondary pulser are switched off. In bake-out-mode, both pulsers are switched off.

Table 3. Maximum power consumption of different operation mode is shown. Nominal values depend on environmental conditions.

Operation Mode	Max. Power / W
GC-Mode	23.0
Bake-Out-Mode	20.0
Exosphere-Mode	19.0
Stand-By	6.8

Comparing similar instruments, power consumption of the NGMS instrument and the RTOF instrument are in a similar range, but overall mass is drastically reduced (see Table 4). The smaller size of the NGMS instrument naturally leads to a reduction in mass. However, the main reason to comply with the mass, size and power allocated to the instrument is improvement in electronics. This reduction in mass establishes landing capabilities on the Moon.

Similar electronic technology is used in the Neutral Gas and Ion Mass spectrometer (NIM) of the Particle and Environment Package (PEP) experiment [17] in ESA's JUICE mission. As the JUICE mission foresees two Europa flybys, where the radiation environment is severe, significant radiation shielding mass has to be employed [18] and accounted for in the mass budget of that system.

Table 4. Evolution of payload budget indicates a trend of miniaturizing. Shown power consumption represents: RTOF mean value and data processing unit, NMS not specified, NGMS maximal value in GC-mode.

Instrument / Mission	Power / W	Mass / kg	Size / cm^3	Reference
RTOF / Rosina /Rosetta	27	14.7	114 x 38 x 24	[3], [21]
NMS / LADEE	36	11.8	-	[19]
NGMS / Luna-Resurs	23	3.5	26 x 15 x 18	-

4. SUMMARY

The built electronic system complies with the challenging mission requirements for a lunar lander. Size, mass, and power consumption of the presented NGMS instrument is unique in space-born mass spectrometers, especially considering the scientific performance of NGMS. Optimization of the ion optical system parameters allows operating at different pressure and temperature ranges with optimized performance. The instrument is capable to adapt to changing thermal environments and covers the full range of possible operation scenarios of GC and exosphere to perform measurement campaigns with high dynamic range. The instrument is capable to perform continuous high-speed data acquisition at a low noise level. An enhanced version of the NGMS electronic system will be part of the NIM instrument to investigate Jupiter's icy moons.

ACKNOWLEDGEMENTS

This project is supported by the Swiss Space Office through the ESA PRODEX program and by the Swiss National Science Foundation. The authors would like to thank the many contributors who made this instrument possible.

REFERENCES

[1] G. Heiken, D. Vaniman, and B. M. French, Lunar sourcebook: A user's guide to the Moon: Cambridge University Press, 1991.

[2] I. Mitrofanov, and L. Zelenyi, "Lunar Landers of Luna-Glob and Luna-Resource missions: science goals and instrumentation." EGU General Assembly Conference Abstracts.

[3] H. Balsiger et al., "Rosina – Rosetta Orbiter Spectrometer for Ion and Neutral Analysis," Space Science Reviews, vol. 128, no. 1-4, pp. 745-801, 2007.

[4] P. Wurz, D. Abplanalp, M. Tulej, M. Iakovleva, V. A. Fernandes, A. Chumikov, and G. G. Managadze, "Mass spectrometric analysis in planetary science: Investigation of the surface and the atmosphere," Solar System Research, vol. 46, no. 6, pp. 408-422, Nov, 2012.

[5] P. Wurz, D. Abplanalp, M. Tulej, and H. Lammer, "A neutral gas mass spectrometer for the investigation of lunar volatiles," Planetary and Space Science, vol. 74, no. 1, pp. 264-269, 2012.

[6] W. C. Wiley, and I. H. McLaren, "Time-of-Flight Mass Spectrometer with Improved Resolution," Review of Scientific Instruments, vol. 26, no. 12, pp. 1150-1157, 1955.

[7] D. Abplanalp, P. Wurz, L. Huber, and I. Leya, "An optimised compact electron impact ion storage source for a time-of-flight mass spectrometer," International Journal of Mass Spectrometry, vol. 294, no. 1, pp. 33-39, Jun 15, 2010.

[8] P. Wurz, and L. Gubler, "Impedance-matching anode for fast timing signals," Review of Scientific Instruments, vol. 65, no. 4, pp. 871-876, 1994.

[9] D. Abplanalp, P. Wurz, L. Huber, I. Leya, E. Kopp, U. Rohner, M. Wieser, L. Kalla, and S. Barabash, "A neutral gas mass spectrometer to measure the chemical composition of the stratosphere," Advances in Space Research, vol. 44, no. 7, pp. 870-878, 2009.

[10] P. Wurz, J. A. Whitby, and G. G. Managadze, "Laser Mass Spectrometry in Planetary Science," AIP Conference Proceedings, vol. 1144, no. 1, pp. 70-75, 2009.

[11] N. Thomas, and G. Cremonese, "The Colour and Stereo Surface Imaging System for ESA's Trace Gas Orbiter." EGU General Assembly Conference Abstracts. p. 3731.

[12] O. W. Richardson, On the Negative Radiation from Hot Platinum: University Press, 1901.

[13] F. W. Wheeler, and W. A. Pearlman, "SPIHT image compression without lists." Acoustics, Speech, and Signal Processing, 2000. ICASSP'00. Proceedings. 2000 IEEE International Conference on. pp. 2047-2050.

[14] L. Hofer et al., "Prototype of the gas chromatograph–mass spectrometer to investigate volatile species in the lunar soil for the Luna-Resurs mission," Planetary and Space Science, vol. 111, pp. 126-133, 2015.

[15] A. Bieler, K. Altwegg, L. Hofer, A. Jackel, A. Riedo, T. Semon, P. Wahlstrom, and P. Wurz, "Optimization of mass spectrometers using the adaptive particle swarm algorithm," J Mass Spectrom, vol. 46, no. 11, pp. 1143-51, Nov, 2011.

[16] Z. H. Zhan, J. Zhang, Y. Li, and H. S. Chung, "Adaptive particle swarm optimization," IEEE Trans Syst Man Cybern B Cybern, vol. 39, no. 6, pp. 1362-81, Dec, 2009.

[17] S. Barabash et al., "Particle Environment Package (PEP)." European Planetary Science Congress 2013, held 8-13 September in London, UK. Online at: http://meetings. copernicus. org/epsc2013, id. EPSC2013-709.

[18] D. Lasi et al., "Shielding an MCP Detector for a Space-Borne Mass Spectrometer Against the Harsh Radiation Environment in Jupiter's Magnetosphere," IEEE Transactions on Nuclear Science, vol. 64, no. 1, pp. 605-613, 2017.

[19] C. T. Russell, and R. C. Elphic, "The Lunar Atmosphere and Dust Environment Explorer Mission Foreword," Space Science Reviews, vol. 185, no. 1-4, pp. 1-2, Dec, 2014.

[20] S. Meyer et al., "Fully automatic and precise data analysis developed for time-of-flight mass spectrometry", Journal of Mass Spectrometry, 2017, 52, 580–590.

[21] S. Scherer et al, "A novel principle for an ion mirror design in time-of-flight mass spectrometry", International Journal of Mass Spectrometry, vol 251, no. 1, pp. 73-81, 2006.

BIOGRAPHY

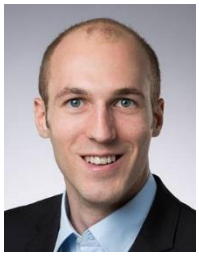

Rico G. Fausch *completed an apprenticeship as technical designer before he received a B.Sc. in Systems Engineering with special qualifications in micro technologies from NTB University of Applied Science (Switzerland) in 2013 and a M.Sc. in Biomedical Engineering from University of Bern (Switzerland) in 2015. He is a Ph.D. student at the Physics Institute at University of Bern, where he is responsible for the scientific and hardware part of the Neutral Gas Mass Spectrometer (NGMS) on board the Roscosmos Luna-Resurs mission. He has experience in the development of devices for electron microscopy sample preparation and liver implants. His research interests include planetary science, sensor technologies and experimental physics.*

Peter Wurz *received a degree in electronic engineering (1985), a M.Sc. and a PhD in Physics at the Technical University of Vienna, Austria (1990). Post-doctoral researcher at Argonne National Laboratory, Chicago, USA. Since 1992 at the University of Bern, Switzerland, habilitation in 1999, since 2003 professor of physics, and since 2015 head of the Space Science and Planetology division. Participation in many space missions of ESA, NASA, ISRO, Roscosmos, and JAXA at co-investigator and principal investigator level.*

Marek Tulej *received a Ph. D. in Physical Chemistry from University of Basel (Switzerland) in 1999 and habilitation (Venia Docendi) from University of Basel (2010) and University of Bern (2011). After his post-doctoral period at Paul Scherrer Insitute (Switzerland) he joined in 2008 the Space Science Group within the Space Research & Planetary Sciences Division, Universtiy of Bern lead by P. Wurz. He has been involved Science Team member in preparation to several space missions including Phobos Ground, Marco Polo-R and currently to Luna-Resurs and JUICE missions.*

Jürg Jost *received a B.Sc. in Electrical Egineering and a M.Sc. in Automation Engineering from Bern University of Applied Sciences (Switzerland) in 1997 and 2003. Since 2001 he leads the electronics group of the Space Research & Planetary Sciences Department, Universtiy of Bern. He managed, designed, built, qualifed and delivered many electronic parts and systems for previous and present space missons like Rosina / ROSETTA, PLASTIC / STEREO, IBEX, P-BACE / MEAP, BELA, ENA and STROFIO / BepiColombo, LASMA / Phobos-Grunt, LASMA-L and NGMS / Luna-Resurs and Luna-Glob, NIM / PEP / JUICE, CaSSIS / Exo-Mars, CHEOPS.*

Pascal Gubler *received a M.Sc. in Information Technology and Electrical Engineering from the Federal Institute of Technology in Zurich (Switzerland) in 2008 and completed a Master of Advanced Studies programme in Management, Technology and Economics in 2012. He has been with the University of Bern since 2011, where he worked as electrical system engineer and FPGA specialist for several space missions as the Laser Mass Spectrometer (LASMA) and the Neugral Gas Mass Spectrometer (NGMS) for the Luna-Resurs and Luna-Glob missions of Roscosmos as well as for the Colour and Stereo Surface Imaging System (CaSSIS) on board the TGO satelite of the ESA Exomars mission.*

Mario Gruber *received a B.Sc. in Computer Science from Bern University of Applied Sciences in 2008. He is experienced as an embedded Software Engineer in research and development for more than 15 years. After working for a national telecommunication provider in Switzerland, he is currently employed at University of Bern and responsible for flight and ground software of the LASMA / Luna-Resurs, NGMS / Luna-Resurs and NIM / JUICE mass-spectrometers and contributed to the success of the CaSSIS telescope on the ExoMars trace gas orbiter TGO.*

Davide Lasi *received a B.Sc. in Chemistry and a M. Sc. in Physical-Chemistry from University of Milano (Italy) in 2004 and 2006, and attended the Stanford Advanced Project Management Certificate Program in 2013. He has been with the University of Bern since 2011, where he worked as project manager for the realization of two mass spectrometers for the Luna-Resurs and Luna-Glob missions of Roscosmos, and the Neutral and Ion Mass Spectrometer part of the Particle Environment Package (PEP) on board ESA mission JUICE. He is currently pursuing a master in System Design and Management at the Massachusetts Institute of Technology.*

Claudio Zimmermann *received a M.Sc. in Electrical Engineering from the Federal Institute of Technology Lausanne (Switzerland, 1998). In its own company he gained large experience in building laser devices for micromachining and developing electronic hardware for aircraft engine control units. He is with the University of Bern since 2013, where he designed and qualified the electronic hardware for the Colour and Stereo Surface Imaging System (CaSSIS) on board the TGO satellite of the ESA Exo-Mars mission.*

Thomas Gerber *received a B.Sc. in Electronics ICT (Information and Communication Technologies) from the Bern University of Applied Sciences (Switzerland) in 2012. He has been with the University of Bern since 2015, where he worked as electrical ingenieur for the CASSIS camera / ESA ExoMars mission and he is currently working for the hardware of the Neutral Gas Mass Spectrometer (NGMS) on board the Roscosmos Luna-Resurs mission.*